

Nucleon electromagnetic form factors with non-local chiral effective Lagrangian

Fangcheng He^{1,2} and P. Wang^{1,3}

¹*Institute of High Energy Physics, CAS, P. O. Box 918(4), Beijing 100049, China*

²*University of Chinese Academy of Sciences, Beijing 100049, China*

³*Theoretical Physics Center for Science Facilities, CAS, Beijing 100049, China*

The relativistic version of finite-range-regularisation is proposed. The covariant regulator is generated from the nonlocal Lagrangian. This nonlocal interaction is gauge invariant and is applied to study the nucleon electromagnetic form factors at momentum transfer up to 2 GeV^2 . Both octet and decuplet intermediate states are included in the one loop calculation. Using a dipole regulator with Λ around 0.85 GeV , the obtained form factors, electromagnetic radii as well as the ratios of the form factors are all comparable with the experimental data. This successful application of chiral effective Lagrangian to relatively large momentum transfer make it possible to further investigation of hadron quantities at high Q^2 .

I. INTRODUCTION

The study of the properties of hadrons continues to attract significant interest in the process of revealing and understanding the essential mechanisms of the strong interactions. The investigation of the electromagnetic form factors of nucleon is very important to help us discover their internal structure. Though QCD is the fundamental theory to describe strong interactions, it is difficult to study hadron physics using QCD directly. There are many phenomenological models, such as the cloudy bag model [1], the constituent quark model [2, 3], the $1/N_c$ expansion approach [4], the perturbative chiral quark model [5], the extended vector meson dominance model [6], the SU(3) chiral quark model [7], the quark-diquark model [8, 9], etc.

Besides the phenomenological models, there are also many lattice-QCD calculations for the electromagnetic form factors [10–16]. Lattice simulation is the most rigorous approach which starts from the first principles. Due to the computing limit, most quantities are still calculated with large quark (π) mass.

In hadron physics, another important method is chiral perturbation theory (ChPT). Heavy baryon and relativistic chiral perturbation theory have been widely applied to study the hadron spectrum and structure. Historically, most formulations of ChPT are based on dimensional or infrared regularisation. Though ChPT is a successful and systematic approach, for the nucleon electromagnetic form factors, it is only valid for $Q^2 < 0.1 \text{ GeV}^2$ [17]. When vector mesons are included, the result is close to the experiments with Q^2 less than 0.4 GeV^2 [18]. Therefore, with traditional ChPT, it is hard to study the form factors at relatively large Q^2 , for example, to explain the G_E/G_M puzzle at large Q^2 .

An alternative regularization method, namely finite-range-regularization (FRR) has been proposed. Inspired by quark models that account for the finite-size of the nucleon as the source of the pion cloud, effective field theory with FRR has been widely applied to extrapolate the vector meson mass, magnetic moments, magnetic form factors, strange form factors, charge radii, first moments of GPDs, nucleon spin, etc [19–34]. In the finite-range-regularization, there is no cut for the energy integral. The regulator is not covariant and is in 3-dimensional momentum space. This non-relativistic regulator can only be applied with the heavy baryon ChPT. A lot of investigations have been done for the finite range regularization and we have good knowledge on the non-relativistic regulator which was kept same for all the above calculations. But we know little about the relativistic regulator and we try to determine the relativistic regulator from the well-known form factors of nucleon.

In this paper, we will provide a relativistic version of FRR. If we simply replace the non-relativistic regulator with a covariant one, the local gauge symmetry and charge conservation will be destroyed. As a result, the renormalized proton (neutron) charge is not 1 (0). Therefore, we generate the covariant regulator from the local gauge invariant Lagrangian. As a result, the nonlocal Lagrangian will be introduced. Using this nonlocal chiral effective Lagrangian, we will study the electromagnetic form factors up to $Q^2 = 2 \text{ GeV}^2$. The paper is organized in the following way. In section II, we briefly introduce the chiral Lagrangian and construct the nonlocal interactions. The matrix elements of the nucleon electromagnetic current is derived in section III. Numerical results are presented in section IV. Finally, section V is a summary.

II. CHIRAL EFFECTIVE LAGRANGIAN

The lowest order chiral Lagrangian for baryons, pseudoscalar mesons and their interaction can be written as [35, 36].

$$\begin{aligned} \mathcal{L} = & i \text{Tr} \bar{B} \gamma_\mu \not{D} B - m_B \text{Tr} \bar{B} B + \bar{T}_\mu^{abc} (i \gamma^{\mu\nu\alpha} D_\alpha - m_T \gamma^{\mu\nu}) T_\nu^{abc} + \frac{f^2}{4} \text{Tr} \partial_\mu \Sigma \partial^\mu \Sigma^\dagger + D \text{Tr} \bar{B} \gamma_\mu \gamma_5 \{A_\mu, B\} \\ & + F \text{Tr} \bar{B} \gamma_\mu \gamma_5 [A_\mu, B] + \left[\frac{\mathcal{C}}{f} \epsilon^{abc} \bar{T}_\mu^{ade} (g^{\mu\nu} + z \gamma_\mu \gamma_\nu) B_c^e \partial_\nu \phi_b^d + H.C. \right], \end{aligned} \quad (1)$$

where D , F and \mathcal{C} are the coupling constants. The chiral covariant derivative \mathcal{D}_μ is defined as $\mathcal{D}_\mu B = \partial_\mu B + [V_\mu, B]$. The pseudoscalar meson octet couples to the baryon field through the vector and axial vector combinations as

$$V_\mu = \frac{1}{2} (\zeta \partial_\mu \zeta^\dagger + \zeta^\dagger \partial_\mu \zeta) + \frac{1}{2} i e \mathcal{A}^\mu (\zeta^+ Q \zeta + \zeta Q \zeta^+), \quad A_\mu = \frac{1}{2} (\zeta \partial_\mu \zeta^\dagger - \zeta^\dagger \partial_\mu \zeta) - \frac{1}{2} e \mathcal{A}^\mu (\zeta Q \zeta^+ - \zeta^+ Q \zeta), \quad (2)$$

where

$$\zeta = e^{i\phi/f}, \quad f = 93 \text{ MeV}. \quad (3)$$

The matrix of pseudoscalar fields ϕ is expressed as

$$\phi = \frac{1}{\sqrt{2}} \begin{pmatrix} \frac{1}{\sqrt{2}} \pi^0 + \frac{1}{\sqrt{6}} \eta & \pi^+ & K^+ \\ \pi^- & -\frac{1}{\sqrt{2}} \pi^0 + \frac{1}{\sqrt{6}} \eta & K^0 \\ K^- & \bar{K}^0 & -\frac{2}{\sqrt{6}} \eta \end{pmatrix}. \quad (4)$$

\mathcal{A}^μ is the photon field. The covariant derivative D_μ in the decuplet part is defined as $D_\nu T_\mu^{abc} = \partial_\nu T_\mu^{abc} + (\Gamma_\nu, T_\mu)^{abc}$, where Γ_ν is the chiral connection [37] defined as $(X, T_\mu) = (X)_d^a T_\mu^{dbc} + (X)_d^b T_\mu^{adc} + (X)_d^c T_\mu^{abd}$. $\gamma^{\mu\nu\alpha}, \gamma^{\mu\nu}$ are the antisymmetric matrices expressed as

$$\gamma^{\mu\nu} = \frac{1}{2} [\gamma^\mu, \gamma^\nu] \quad \text{and} \quad \gamma^{\mu\nu\rho} = \frac{1}{4} \{[\gamma^\mu, \gamma^\nu], \gamma^\rho\} \quad (5)$$

In the chiral $SU(3)$ limit, the octet and decuplet baryons will have the same mass m_B and m_T . In our calculation, we use the physical masses for baryon octets and decuplets. The explicit form of the baryon octet is written as

$$B = \begin{pmatrix} \frac{1}{\sqrt{2}} \Sigma^0 + \frac{1}{\sqrt{6}} \Lambda & \Sigma^+ & p \\ \Sigma^- & -\frac{1}{\sqrt{2}} \Sigma^0 + \frac{1}{\sqrt{6}} \Lambda & n \\ \Xi^- & \Xi^0 & -\frac{2}{\sqrt{6}} \Lambda \end{pmatrix}. \quad (6)$$

For the baryon decuplets, there are three indices, defined as

$$\begin{aligned} T_{111} &= \Delta^{++}, \quad T_{112} = \frac{1}{\sqrt{3}} \Delta^+, \quad T_{122} = \frac{1}{\sqrt{3}} \Delta^0, \\ T_{222} &= \Delta^-, \quad T_{113} = \frac{1}{\sqrt{3}} \Sigma^{*,+}, \quad T_{123} = \frac{1}{\sqrt{6}} \Sigma^{*,0}, \\ T_{223} &= \frac{1}{\sqrt{3}} \Sigma^{*,-}, \quad T_{133} = \frac{1}{\sqrt{3}} \Xi^{*,0}, \quad T_{233} = \frac{1}{\sqrt{3}} \Xi^{*,-}, \quad T_{333} = \Omega^-. \end{aligned} \quad (7)$$

The octet, decuplet and octet-decuplet transition magnetic moment operators are needed in the one loop calculation of nucleon electromagnetic form factors. The baryon octet anomalous magnetic Lagrangian is written as

$$\mathcal{L} = \frac{e}{4m_N} (c_1 \text{Tr} \bar{B} \sigma^{\mu\nu} \{F_{\mu\nu}^+, B\} + c_2 \text{Tr} \bar{B} \sigma^{\mu\nu} [F_{\mu\nu}^+, B]), \quad (8)$$

where

$$F_{\mu\nu}^+ = -\frac{1}{2} (\zeta^\dagger F_{\mu\nu} Q \zeta + \zeta F_{\mu\nu} Q \zeta^\dagger). \quad (9)$$

The transition magnetic operator is

$$\mathcal{L} = i \frac{e}{4m_N} \mu_T F_{\mu\nu} (\epsilon_{ijk} Q_j^i \bar{B}_m^j \gamma^\mu \gamma_5 T^{\nu,klm} + \epsilon^{ijk} Q_i^l \bar{T}_{klm}^\mu \gamma^\nu \gamma_5 B_j^m), \quad (10)$$

where the matrix Q is defined as $Q = \text{diag}\{2/3, -1/3, -1/3\}$. At the lowest order, the Lagrangian will generate the following nucleon anomalous magnetic moments:

$$F_2^p = \frac{1}{3}c_1 + c_2, \quad F_2^n = -\frac{2}{3}c_1. \quad (11)$$

In quark model, the nucleon magnetic moments can be written in terms of quark magnetic moments. For example, $\mu_p = \frac{4}{3}\mu_u - \frac{1}{3}\mu_d$, $\mu_n = \frac{4}{3}\mu_d - \frac{1}{3}\mu_u$. Using $\mu_u = -2\mu_d = 2\mu_s$, we can get the following relationships

$$c_1 = \frac{3}{2}(c_2 + 1), \quad c_1 = \frac{3}{2}\mu_u, \quad \mu_T = 4c_1 \quad (12)$$

The effective decuplet anomalous magnetic moment operator can be expressed as effective Lagrangian

$$\mathcal{L} = -\frac{ieF_2^T}{2m_T} \bar{T}_\mu^{abc} \sigma^{\rho\sigma} q_\sigma \mathcal{A}_\rho T_\mu^{abc}. \quad (13)$$

For each decuplet baryon, its moment F_2^T can be written in terms of c_1 . For example, for Δ^{++} , the magnetic moment $\mu_{\Delta^{++}} = 3\mu_u = 2c_1$. Therefore, $F_2^{\Delta^{++}} = 2c_1 - 2$. In our numerical calculations, the above anomalous magnetic moments of baryons at tree level which only depend on the parameter c_1 are used.

Now we construct the nonlocal Lagrangian which will generate the covariant regulator. The gauge invariant nonlocal Lagrangian can be obtained using the method in [38–40]. For instance, the local interaction including π meson can be written as

$$\mathcal{L}_\pi^{\text{local}} = \int dx \frac{D+F}{\sqrt{2}f} \bar{p}(x) \gamma^\mu \gamma_5 n(x) (\partial_\mu + ie \mathcal{A}_\mu(x)) \pi^+(x). \quad (14)$$

The nonlocal Lagrangian for this interaction is expressed as

$$\begin{aligned} \mathcal{L}_\pi^{\text{nl}} = & \int dx \int dy \frac{D+F}{\sqrt{2}f} \bar{p}(x) \gamma^\mu \gamma_5 n(x) F(x-y) \exp[ie \int_x^y dz_\nu \int da \mathcal{A}^\nu(z-a) F(a)] \\ & \times (\partial_\mu + ie \int da \mathcal{A}_\mu(y-a) F(a)) \pi^+(y), \end{aligned} \quad (15)$$

where $F(x)$ is the correlation function. To guarantee the gauge invariance, the gauge link is introduced in the above Lagrangian. The regulator can be generated automatically with correlation function. With the same idea, the nonlocal electromagnetic interaction can also be obtained. For example, the local interaction between proton and photon is written as

$$\mathcal{L}_{EM}^{\text{local}} = -e \bar{p}(x) \gamma^\mu p(x) \mathcal{A}_\mu(x) + \frac{(c_1-1)e}{4m_N} \bar{p}(x) \sigma^{\mu\nu} p(x) F_{\mu\nu}(x). \quad (16)$$

The corresponding nonlocal Lagrangian is expressed as

$$\mathcal{L}_{EM}^{\text{nl}} = -e \int da \bar{p}(x) \gamma^\mu p(x) \mathcal{A}_\mu(x-a) F_1(a) + \frac{(c_1-1)e}{4m_N} \int da \bar{p}(x) \sigma^{\mu\nu} p(x) F_{\mu\nu}(x-a) F_2(a), \quad (17)$$

where $F_1(a)$ and $F_2(a)$ is the correlation function for the nonlocal electric and magnetic interactions. The form factors at tree level which are momentum dependent can be easily obtained with the Fourier transformation. The simplest choice is to assume that the correlation function of the nucleon electromagnetic vertex is the same as that of the nucleon-pion vertex, i.e. $F_1(a) = F_2(a) = F(a)$. Therefore, the Dirac and Pauli form factors will have the same dependence on the momentum transfer at tree level. As a result, the obtained charge form factor of proton decreases very quickly with increasing Q^2 and it will become negative after some Q^2 . The better choice is to assume that the charge and magnetic form factors at tree level have the same the momentum dependence as nucleon-pion vertex, i.e. $G_M^{\text{tree}}(p) = c_1 G_E^{\text{tree}}(p) = c_1 \tilde{F}(p)$, where $\tilde{F}(p)$ is the Fourier transformation of the correlation function $F(a)$. The

corresponding function of $\tilde{F}_1(q)$ and $\tilde{F}_2(q)$ is then expressed as

$$\tilde{F}_1^p(q) = \tilde{F}(q) \frac{4m_N^2 + c_1 Q^2}{4m_N^2 + Q^2}, \quad \tilde{F}_2^p(q) = \tilde{F}(q) \frac{4m_N^2}{4m_N^2 + Q^2}, \quad (18)$$

From the above equations, one can see that in the heavy baryon limit, these two choices are equivalent. The nonlocal Lagrangian is invariant under the following gauge transformation

$$\pi^+(y) \rightarrow e^{i\alpha(y)} \pi^+(y), \quad p(x) \rightarrow e^{i\alpha(x)} p(x), \quad \mathcal{A}_\mu(x) \rightarrow \mathcal{A}_\mu(x) - \frac{1}{e} \partial_\mu \alpha'(x), \quad (19)$$

where $\alpha(x) = \int da \alpha'(x-a) F(a)$. From Eq. (15), two kinds of couplings between hadrons and one photon can be obtained. One is the normal interaction expressed as

$$\mathcal{L}^{nor} = ie \int dx \int dy \frac{D+F}{\sqrt{2}f} \bar{p}(x) \gamma^\mu \gamma_5 n(x) F(x-y) \pi^+(y) \int da \mathcal{A}_\mu(y-a) F(a), \quad (20)$$

This interaction is similar as the traditional local Lagrangian except the correlation function. The other one is the additional interaction obtained by the expansion of the gauge link, expressed as

$$\mathcal{L}^{add} = ie \int dx \int dy \frac{D+F}{\sqrt{2}f} \bar{p}(x) \gamma^\mu \gamma_5 n(x) F(x-y) \int_x^y dz_\nu \int da \mathcal{A}^\nu(z-a) F(a) \partial_\mu \pi^+(y) \quad (21)$$

The additional interaction is important to get the renormalized proton (neutron) charge 1 (0). The Feynman rules for the nonlocal Lagrangian are listed in the Appendix.

III. ELECTROMAGNETIC FORM FACTORS

The Dirac and Pauli form factors are defined as

$$\langle N(p') | J_\mu | N(p) \rangle = \bar{u}(p') \left\{ \gamma^\mu F_1^N(Q^2) + \frac{i\sigma^{\mu\nu} q_\nu}{2m_N} F_2^N(Q^2) \right\} u(p), \quad (22)$$

where $q = p' - p$ and $Q^2 = -q^2$. $F_1^N(Q^2)$ and $F_2^N(Q^2)$ are the Dirac and Pauli form factors. The combination of the above form factors can generate the electric and magnetic form factors as

$$G_E^N(Q^2) = F_1^N(Q^2) - \frac{Q^2}{4m_N^2} F_2^N(Q^2) \quad G_M^N(Q^2) = F_1^N(Q^2) + F_2^N(Q^2) \quad (23)$$

Charge and magnetic radii are defined by

$$\langle (r_E^p)^2 \rangle = \frac{-6}{G_E^p(0)} \frac{dG_E^p(Q^2)}{dQ^2} \Big|_{Q^2=0}, \quad \langle (r_M^p)^2 \rangle = \frac{-6}{G_M^p(0)} \frac{dG_M^p(Q^2)}{dQ^2} \Big|_{Q^2=0}, \quad (24)$$

$$\langle (r_E^n)^2 \rangle = -6 \frac{dG_E^n(Q^2)}{dQ^2} \Big|_{Q^2=0}, \quad \langle (r_M^n)^2 \rangle = \frac{-6}{G_M^n(0)} \frac{dG_M^n(Q^2)}{dQ^2} \Big|_{Q^2=0}. \quad (25)$$

According to the Lagrangian, the one loop Feynman diagrams which contribute to the nucleon electromagnetic form factors are plotted in Fig. 1.

In this section, we will only show the expressions for the intermediate octet baryon part. For the intermediate decuplet baryon part, the expressions are written in the Appendix. In diagram Fig. 1a, the photon couples to the meson. The contribution of Fig. 1a to the matrix element in Eq. (22) is expressed as

$$\Gamma_a^{\mu(p)} = -(D+F)^2 I_{a\pi}^N - \frac{(3F+D)^2}{6} I_{aK}^\Lambda - \frac{(D-F)^2}{2} I_{aK}^\Sigma, \quad (26)$$

$$\Gamma_a^{\mu(n)} = (D+F)^2 I_{a\pi}^N - (D-F)^2 I_{aK}^\Sigma, \quad (27)$$

where $I_{a\pi}^N$, I_{aK}^Λ and I_{aK}^Σ are the integrals for the $N\pi$, ΛK and ΣK intermediate states, respectively. $I_{a\pi}^N$ is expressed

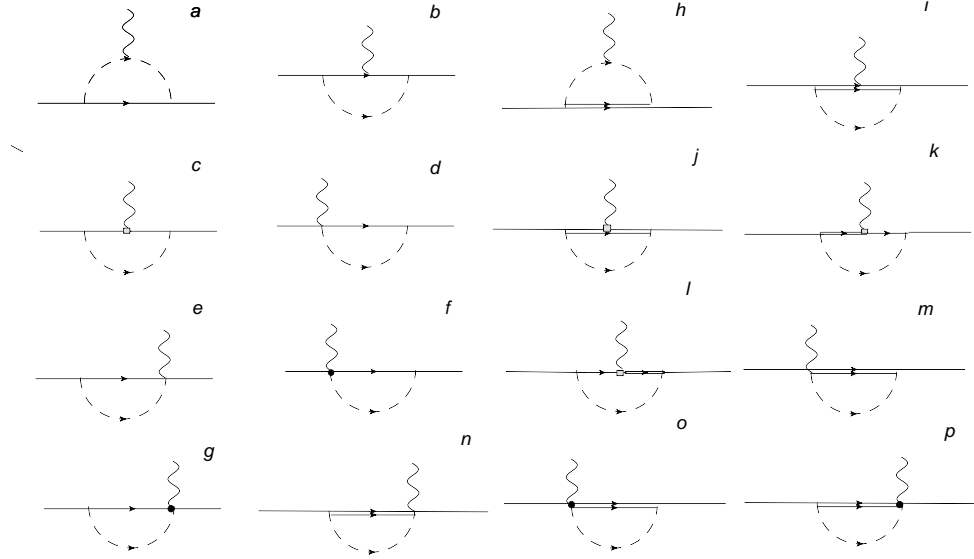


FIG. 1: One-loop Feynman diagrams for the nucleon electromagnetic form factors. The solid, double-solid, dashed and wave lines are for the octet baryons, decuplet baryons, pseudoscalar mesons and photons, respectively. The rectangle and blackdot represent magnetic and additional interacting vertex.

as

$$I_{a\pi}^N = \bar{u}(p') \int \frac{d^4k}{(2\pi)^4} \frac{(\not{k} + \not{q})\gamma_5}{\sqrt{2}f} \tilde{F}(q+k) \frac{1}{D_\pi(k+q)} (2k+q)^\mu \frac{1}{D_\pi(k)} \frac{1}{\not{p} - \not{k} - m_N} \frac{-\not{k}\gamma_5}{\sqrt{2}f} \tilde{F}(k) u(p). \quad (28)$$

$D_\pi(k)$ is given by

$$D_\pi(k) = k^2 - M_k^2 + i\epsilon. \quad (29)$$

The expressions for I_{aK}^Λ and I_{aK}^Σ are the same except the intermediate meson and baryon masses are changed to be those of K meson and hyperons. For simplicity, we will only show the expression for the π meson case.

In Fig.1b, the photon couples to the intermediate baryon with electric vertex. The contribution of this diagram with octet intermediate baryons is expressed as

$$\begin{aligned} \Gamma_b^{\mu(p)} = & \frac{1}{2}(D+F)^2 \frac{12m_p^2 - c_1Q^2}{12m_p^2 + 3Q^2} I_{b\pi}^{NN} + \frac{(3F-D)^2}{6} \frac{4m_p^2 + c_1Q^2}{4m_p^2 + Q^2} I_{b\eta}^{NN} + (D-F)^2 \frac{24m_\Sigma^2 + 7c_1Q^2}{24m_\Sigma^2 + 6Q^2} I_{bK}^{N\Sigma} \\ & - \frac{(3F+D)^2}{18} \frac{c_1Q^2}{4m_\Lambda^2 + Q^2} I_{bK}^{N\Lambda} - \frac{(3F+D)(D-F)}{3} \frac{c_1Q^2}{4m_\Sigma^2 + Q^2} I_{bK}^{N\Lambda\Sigma}, \end{aligned} \quad (30)$$

$$\begin{aligned} \Gamma_b^{\mu(n)} = & (D+F)^2 \frac{12m_p^2 + 2c_1Q^2}{12m_p^2 + 3Q^2} I_{b\pi}^{NN} - \frac{(3F-D)^2}{9} \frac{c_1Q^2}{4m_p^2 + Q^2} I_{b\eta}^{NN} - \frac{(3F+D)^2}{18} \frac{c_1Q^2}{4m_\Lambda^2 + Q^2} I_{bK}^{N\Lambda} \\ & - (D-F)^2 \frac{c_1Q^2 + 24m_\Sigma^2}{24m_\Sigma^2 + 6Q^2} I_{bK}^{N\Sigma} + \frac{(3F+D)(D-F)}{3} \frac{c_1Q^2}{4m_\Sigma^2 + Q^2} I_{bK}^{N\Lambda\Sigma}, \end{aligned} \quad (31)$$

where the integral $I_{b\pi}^{NN}$ is written as

$$I_{b\pi}^{NN} = \tilde{F}(q) \bar{u}(p') \int \frac{d^4k}{(2\pi)^4} \frac{\not{k}\gamma_5}{\sqrt{2}f} \tilde{F}(k) \frac{1}{D_\pi(k)} \frac{1}{\not{p}' - \not{k} - m_N} (-\gamma_\mu) \frac{1}{\not{p} - \not{k} - m_N} \frac{-\not{k}\gamma_5}{\sqrt{2}f} \tilde{F}(k) u(p). \quad (32)$$

Fig.1c is for the magnetic baryon-photon interaction. The contribution of this diagram is expressed as

$$\begin{aligned}\Gamma_c^{\mu(p)} &= -\frac{(4c_1 + 12)m_p^2}{12m_p^2 + 3Q^2}(D + F)^2 I_{c\pi}^{NN} + \frac{(4c_1 - 4)m_p^2}{12m_p^2 + 3Q^2}(3F - D)^2 I_{c\eta}^{NN} - \frac{4c_1 m_\Lambda^2}{36m_\Lambda^2 + 9Q^2}(3F + D)^2 I_{cK}^{N\Lambda} \\ &+ \frac{(28c_1 - 24)m_\Sigma^2}{12m_\Sigma^2 + 3Q^2}(D - F)^2 I_{cK}^{N\Sigma} - \frac{8c_1(D - F)(3F + D)m_\Sigma^2}{12m_\Sigma^2 + 3Q^2} I_{cK}^{N\Lambda\Sigma},\end{aligned}\quad (33)$$

$$\begin{aligned}\Gamma_c^{\mu(n)} &= \frac{(16c_1 - 24)m_p^2}{12m_p^2 + 3Q^2}(D + F)^2 I_{c\pi}^{NN} - \frac{8c_1 m_N^2}{36m_N^2 + 9Q^2}(3F - D)^2 I_{c\eta}^{NN} - \frac{4c_1 m_\Lambda^2}{36m_\Lambda^2 + 9Q^2}(3F + D)^2 I_{cK}^{N\Lambda} \\ &- \frac{(4c_1 - 24)m_\Sigma^2}{12m_\Sigma^2 + 3Q^2}(D - F)^2 I_{cK}^{N\Sigma} + \frac{8c_1(D - F)(3F + D)m_\Sigma^2}{12m_\Sigma^2 + 3Q^2} I_{cK}^{N\Lambda\Sigma},\end{aligned}\quad (34)$$

where

$$I_{c\pi}^{NN} = \tilde{F}(q)\bar{u}(p') \int \frac{d^4 k}{(2\pi)^4} \frac{\not{k}\gamma_5}{2f} \tilde{F}(k) \frac{1}{\not{p}' - \not{k} - m_N} \frac{\sigma^{\mu\nu} q_\nu}{2m_N} \frac{1}{\not{p} - \not{k} - m_N} \frac{i}{D_\pi(k)} \frac{\not{k}\gamma_5}{2f} \tilde{F}(k) u(p). \quad (35)$$

$$(36)$$

The contribution from Fig. 1d+1e is written as

$$\Gamma_{d+e}^{\mu(p)} = -(D + F)^2 I_{(d+e)\pi}^{NN} - \frac{(3F + D)^2}{6} I_{(d+e)K}^{N\Lambda} - \frac{(D - F)^2}{2} I_{(d+e)K}^{N\Sigma}, \quad (37)$$

$$\Gamma_{d+e}^{\mu(n)} = (D + F)^2 I_{(d+e)\pi}^{NN} - (D - F)^2 I_{(d+e)K}^{N\Sigma}, \quad (38)$$

where

$$\begin{aligned}I_{(d+e)\pi}^{NN} &= \tilde{F}(q)\bar{u}(p') \int \frac{d^4 k}{(2\pi)^4} \frac{\not{k}\gamma_5}{\sqrt{2}f} \tilde{F}(k) \frac{1}{\not{p}' - \not{k} - m} \frac{1}{D_\pi(k)} \frac{-1}{\sqrt{2}f} \gamma^\mu \gamma_5 \tilde{F}(q - k) u(p) \\ &+ \tilde{F}(q)\bar{u}(p') \int \frac{d^4 k}{(2\pi)^4} \frac{1}{\sqrt{2}f} \gamma^\mu \gamma_5 \tilde{F}(q + k) \frac{1}{\not{p} - \not{k} - m} \frac{1}{D_\pi(k)} \frac{-\not{k}\gamma_5}{\sqrt{2}f} \tilde{F}(k) u(p).\end{aligned}\quad (39)$$

These two diagrams only have contribution in the relativistic cases. In the heavy baryon limit, they have no contribution to either electric or magnetic form factors.

Fig. 1f and 1g are the additional diagrams which generated from the expansion of the gauge link terms. They are important to get the renormalized charge to proton (neutron) to be 1 (0). The contribution of these two additional diagrams with intermediate octet baryons is expressed as

$$\Gamma_{f+g}^{\mu(p)} = -(D + F)^2 I_{(f+g)\pi}^{NN} - \frac{(3F + D)^2}{6} I_{(f+g)K}^{N\Lambda} - \frac{(D - F)^2}{2} I_{(f+g)K}^{N\Sigma}, \quad (40)$$

$$\Gamma_{f+g}^{\mu(n)} = (D + F)^2 I_{(f+g)\pi}^{NN} - (D - F)^2 I_{(f+g)K}^{N\Sigma}, \quad (41)$$

where

$$\begin{aligned}I_{(f+g)\pi}^{NN} &= \tilde{F}(q)\bar{u}(p') \int \frac{d^4 k}{(2\pi)^4} \frac{\not{k}\gamma_5}{\sqrt{2}f} \tilde{F}(k) \frac{1}{\not{p}' - \not{k} - m} \frac{1}{D_\pi(k)} \frac{1}{\sqrt{2}f} (-\not{k}\gamma_5) \frac{(-2k + q)^\mu}{-2kq + q^2} [\tilde{F}(k - q) - \tilde{F}(k)] u(p) \\ &+ \tilde{F}(q)\bar{u}(p') \int \frac{d^4 k}{(2\pi)^4} \frac{1}{\sqrt{2}f} \not{k}\gamma_5 \frac{(2k + q)^\mu}{2kq + q^2} [\tilde{F}(k + q) - \tilde{F}(k)] \frac{1}{\not{p} - \not{k} - m} \frac{1}{D_\pi(k)} \frac{\not{k}\gamma_5}{\sqrt{2}f} \tilde{F}(k) u(p).\end{aligned}\quad (42)$$

Using FeynCalc to simplify the γ matrix algebra, we can get the separate expressions for the Dirac and Pauli form factors. Numerical results will be discussed in the next section.

IV. NUMERICAL RESULTS

In the numerical calculations, the parameters are chosen as $D = 0.76$ and $F = 0.50$ ($g_A = D + F = 1.26$). The coupling constant \mathcal{C} is chosen to be 1 which is the same as in Ref. [41]. The off-shell parameter z is chosen to be $z = -1$ [42]. The low energy constant c_1 is fitted by the experimental moment of $F_2^n(0) = -1.91$. The covariant

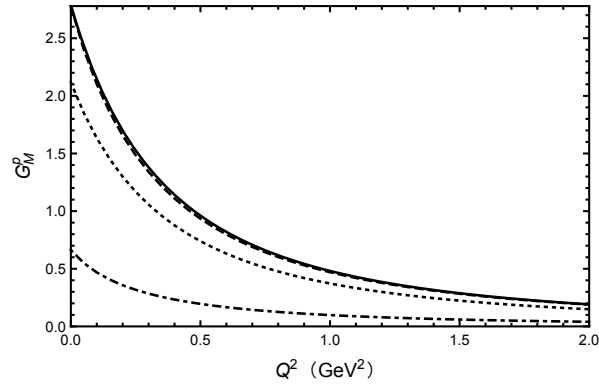


FIG. 2: The proton magnetic form factor versus momentum transfer Q^2 with $\Lambda = 0.85$ GeV. The solid line is for the empirical result. The dotted, dot-dashed and dashed lines are for the tree, loop and total contribution, respectively.

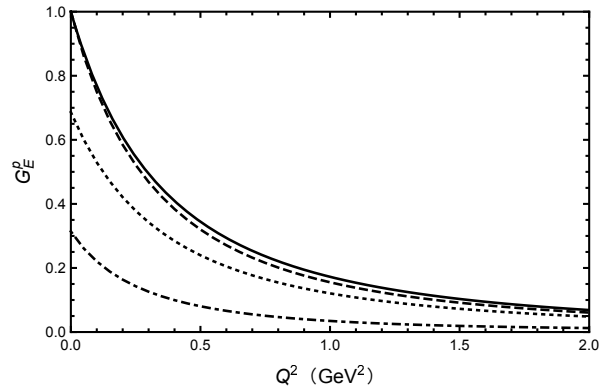


FIG. 3: Same as Fig. 2 but for the proton electric form factor.

regulator is chosen to be of a dipole form

$$\tilde{F}(k) = \frac{1}{(1 - k^2/\Lambda^2)^2}, \quad (43)$$

where Λ is the only free parameter. By varying the value of Λ , we found when Λ is around 0.85 GeV, the results are very close to the experimental nucleon form factors.

The calculated proton magnetic form factor $G_M^p(Q^2)$ versus Q^2 is plotted in Fig. 2. The solid line is for the empirical result with $G_M^p(Q^2) = 2.79/(1 + Q^2/0.71 \text{ GeV}^2)^2$. The dotted, dot-dashed and dashed lines are for the tree, loop and total contribution, respectively. As we explained previously, on the one hand, the nonlocal Lagrangian generates the covariant regulator which makes the loop integral convergent. On the other hand, it also generates the Q^2 dependent contribution at tree level. Compared with the conventional ChPT, the tree level contribution is not expanded in powers of momentum transfer. As a result, both the tree and loop contribution decrease smoothly with the increasing Q^2 and the total obtained form factor is close to the experimental value up to $Q^2 = 2 \text{ GeV}^2$. For $Q^2 = 0$, the contribution to μ^p at tree level is 2.11 and the loop contribution to μ^p is 0.67. The total μ^p is 2.78. This proton magnetic moment is calculated with fixed c_1 which is determined by the neutron magnetic moment ($\mu^n = -1.91$). The proton magnetic radii is 0.848 fm in our calculation, which is obviously close to the experimental value.

The proton charge form factor versus Q^2 is shown in Fig 3. The solid, dashed, dotted and dot-dashed lines have the same meaning as Fig. 2 except for the charge form factor. From the figure, one can see both the tree and loop contribution are important to get the correct Q^2 dependence of the form factors. At $Q^2 = 0$, the sum of the tree and loop contribution to proton charge is 1. The additional diagrams generated from the expansion of the gauge link is crucial to get the renormalized proton charge 1. Compared with the magnetic form factor, the charge form factor decreases faster. As a result, the obtained charge radii 0.857 fm is a little larger than the magnetic radii

The neutron magnetic form factor versus Q^2 is shown in Fig. 4. Similar as the proton case, the solid line is for

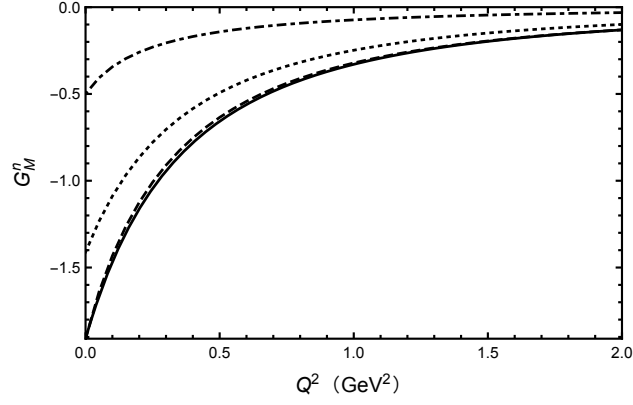


FIG. 4: The magnetic form factor of neutron versus momentum transfer Q^2 with $\Lambda = 0.85$ GeV. The solid line is for the empirical result. The dotted, dot-dashed and dashed lines are for the tree, loop and total contribution, respectively.

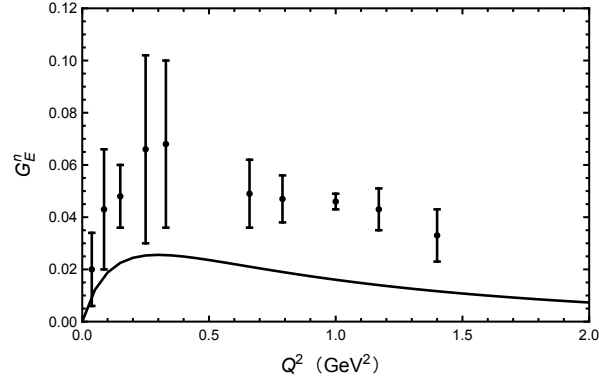


FIG. 5: The electric form factor of neutron versus momentum transfer Q^2 with $\Lambda = 0.85$ GeV. The experimental data is from [43].

the empirical result. The dotted, dot-dashed and dashed lines represent the tree, loop and total contribution to the neutron form factor, respectively. Again, compared with the empirical data, our calculated result is very good up to $Q^2 = 2$ GeV². The calculated magnetic radii of neutron is 0.867 fm. From Fig. 2 to Fig. 4, we can see the loop diagrams contribute about 25%–30% to proton electromagnetic form factors and neutron magnetic form factor, while 70%–75% of the form factors is from the tree level contribution.

The neutron charge form factor is plotted in Fig 5. Since the charge of neutron is 0, all the contribution to the neutron charge form factor is from the loop. It first increases and then decreases with the increasing momentum transfer. The neutron charge radii $\langle (r_M^n)^2 \rangle = -0.077$ fm², which is smaller than experimental value -0.11 fm². Though the calculated charge form factor of neutron is smaller than experimental values, overall the result is still reasonable.

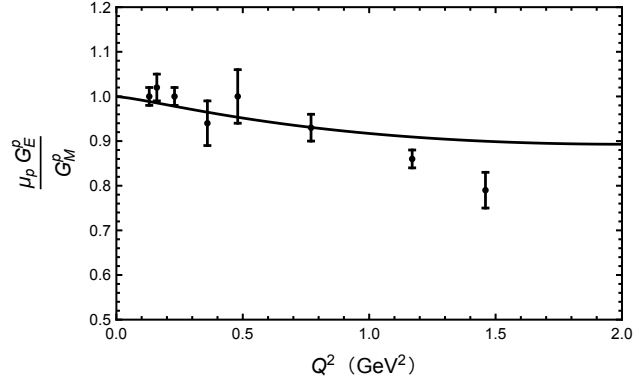


FIG. 6: Ratio of proton electric to normalized magnetic form factor versus momentum transfer Q^2 . Experimental result is from [44]

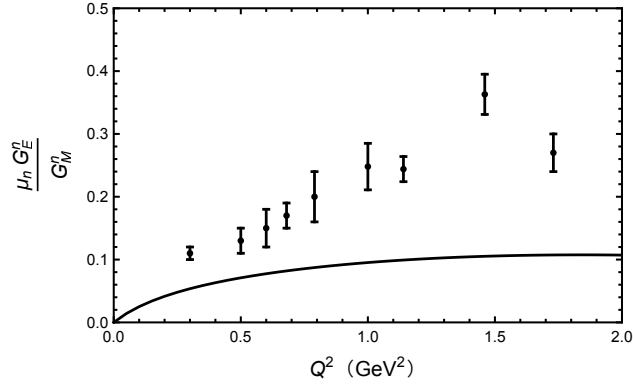


FIG. 7: Ratio of neutron electric to normalized magnetic form factor versus momentum transfer Q^2 . Experimental result is from [45]

In the traditional ChPT, in addition to the two parameters c_1 and c_2 which were determined by the proton and neutron magnetic moments, there are four other parameters fitted by the electric and magnetic radii of proton and neutron. Here besides the parameter c_1 fitted by the experimental neutron magnetic moment, we have only one free parameter Λ in the regulator. The proton magnetic moment and the nucleon radii are calculated instead of fitted. With fewer parameters, the obtained electromagnetic form factors of proton and neutron are all much better than those in the traditional ChPT. This makes it possible to study the form factors precisely at relatively large Q^2 .

With the precisely determined form factors, we now show the ratios of the electric to normalized magnetic form factor. The ratio for proton is plotted in Fig 6. If without loop contribution, the ratio will remain to be 1 for all Q^2 . With loop contribution, $\frac{\mu_p G_E^p}{G_M^p}$ automatically decreases with the increasing Q^2 . Our calculated result is comparable with the experimental data, though at large Q^2 , the experimental data drop more quickly.

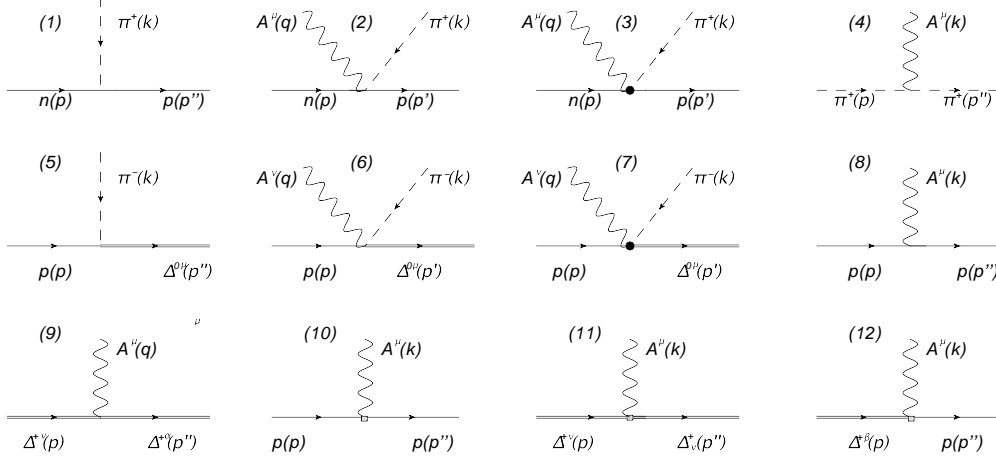
The ratio for neutron is plotted in Fig 7. From the figure, one can see the ratio $\frac{\mu_n G_E^n}{G_M^n}$ increases with the increasing Q^2 as the experimental data. This is purely due to the loop contribution. The experimental ratio of $\frac{\mu_n G_E^n}{G_M^n}$ increases more quickly than our result. It is mainly because our calculated G_E^n is smaller than the experimental data.

V. SUMMARY

We proposed a relativistic version for the finite-range-regularization which makes it possible to study the hadron properties with relativistic chiral effective Lagrangian at large Q^2 . The finite-range-regularization has been widely applied to investigate the nucleon mass, form factors, electromagnetic radii, generalized parton distributions, proton spin, etc. We have good knowledge on the 3-dimensional regulator which was kept the same for all the calculations.

TABLE I: The parameters and calculated magnetic moments and electromagnetic radii of nucleon

Λ (GeV)	Z	c_1	μ_p	μ_n	r_{Mp} (fm)	r_{Ep} (fm)	r_{Mn} (fm)	r_{En}^2 (fm ²)
0.8	0.71	3.090	2.78	-1.91	0.893	0.903	0.912	-0.076
0.85	0.69	3.085	2.78	-1.91	0.848	0.857	0.867	-0.077
0.9	0.66	3.077	2.78	-1.91	0.808	0.816	0.829	-0.082
Exp.	-	-	2.79	-1.91	0.836	0.847	0.889	-0.113

FIG. 8: The interacting vertex in the calculation of nucleon form factors. Only the π case is shown as an example. The rectangle and black dot represent the magnetic and additional interacting vertex.

However, we have little knowledge on the covariant 4-dimensional regulator. Therefore, we start from the well-determined nucleon form factors and it was found that using the dipole regulator with Λ around 0.85 GeV the nucleon form factors can be described very well up to $Q^2 = 2$ GeV². The covariant regulator is generated from the nonlocal gauge invariant Lagrangian. As a result, the renormalized charge of proton (neutron) is 1 (0) with the additional diagrams obtained by the expansion of the gauge link. The nonlocal interaction generates both the regulator which makes the loop integral convergent and the Q^2 dependence of form factors at tree level. In this approach, we have only two parameters c_1 and Λ instead of six parameters in the traditional ChPT. With fewer parameters, our calculated form factors are much better. The ratios of the electric to normalized magnetic form factor are also comparable with the experimental data. From our calculation, the G_N^E/G_N^M puzzle can be naturally understood. This is the first time to calculate the form factors precisely at relatively large Q^2 with chiral effective Lagrangian. The successful application of chiral effective Lagrangian to large momentum transfer will be very helpful for us to investigate hadron quantities at high Q^2 . As a summary, we list the parameters and obtained magnetic moments and electromagnetic radii in Table I.

Acknowledgments

This work is supported by NSFC under Grant No. 11475186, by DFG and NSFC (CRC 110) and by Key Research Program of Frontier Sciences, CAS under Grant NO. Y7292610K1.

Appendix

The Feynman rules for the nonlocal vertexes are written as

$$\begin{aligned}
(1) & : \frac{\not{k}\gamma_5}{\sqrt{2}f}(D+F)\tilde{F}(k) \\
(2) & : -\frac{e}{\sqrt{2}f}(D+F)\gamma^\mu\gamma_5\tilde{F}(k+q)\tilde{F}(q) \\
(3) & : -\frac{e}{\sqrt{2}f}\not{k}\gamma_5\frac{(2k+q)^\mu}{2kq+q^2}[\tilde{F}(k+q)-\tilde{F}(k)]\tilde{F}(q) \\
(4) & : -ie(p+p'')^\mu\tilde{F}(q) \\
(5) & : -\frac{\mathcal{C}}{\sqrt{6}f}(k_\mu+z\gamma_\mu\not{k})\tilde{F}(k) \\
(6) & : -\frac{e\mathcal{C}}{\sqrt{6}f}(g^{\nu\mu}+z\gamma^\mu\gamma^\nu)\tilde{F}(k+q)\tilde{F}(q) \\
(7) & : -\frac{e\mathcal{C}}{\sqrt{6}f}(k_\mu+z\gamma_\mu\not{k})\frac{(2k+q)^\mu}{2kq+q^2}[\tilde{F}(k+q)-\tilde{F}(k)]\tilde{F}(q) \\
(8) & : -ie\gamma^\mu\frac{4m_N^2+c_1Q^2}{4m_N^2+Q^2}\tilde{F}(q) \\
(9) & : -ie\gamma^{\alpha\nu\mu}\frac{4m_\Delta^2+c_1Q^2}{4m_\Delta^2+Q^2}\tilde{F}(q) \\
(10) & : \frac{4e(c_1-1)m_N^2}{4m_N^2+Q^2}\frac{\sigma^{\mu\nu}q_\nu}{2m_N}\tilde{F}(q) \\
(11) & : -\frac{4e(c_1-1)m_\Delta^2}{4m_\Delta^2+Q^2}\frac{\sigma^{\mu\lambda}q_\lambda}{2m_\Delta}\tilde{F}(q) \\
(12) & : e\frac{\sqrt{3}}{3m_N}c_1F_{\mu\nu}\gamma^\mu\gamma_5\tilde{F}(q)
\end{aligned}$$

The expressions for the decuplet part are written in the following way. The contribution of Fig. 1h is expressed as

$$\Gamma_h^{\mu(p)} = \frac{2\mathcal{C}^2}{3}I_{h\pi}^{N\Delta} - \frac{\mathcal{C}^2}{6}I_{hK}^{N\Sigma^*}, \quad (44)$$

$$\Gamma_h^{\mu(n)} = -\frac{2\mathcal{C}^2}{3}I_{h\pi}^{N\Delta} - \frac{\mathcal{C}^2}{3}I_{hK}^{N\Sigma^*}, \quad (45)$$

where

$$\begin{aligned}
I_{h\pi}^{N\Delta} & = \bar{u}(p') \int \frac{d^4k}{(2\pi)^4} \frac{1}{2f^2} ((k+q)_\sigma + z(\not{k} + \not{q})\gamma_\sigma) F(q+k) \frac{1}{D_\pi(k+q)} \\
& \times e(2k+q)^\mu \frac{1}{D_\pi(k)} \frac{1}{\not{p} - \not{k} - m_\Delta} S_{\sigma\rho}(-k_\rho - z\gamma_\rho\not{k}) F(k) u(p).
\end{aligned} \quad (46)$$

$S_{\sigma\rho}$ is expressed as

$$S_{\sigma\rho} = -g_{\sigma\rho} + \frac{\gamma_\sigma\gamma_\rho}{3} + \frac{2(p-k)_\sigma(p-k)_\rho}{3m_\Delta^2} + \frac{\gamma_\sigma(p-k)_\rho - \gamma_\rho(p-k)_\sigma}{3m_\Delta}. \quad (47)$$

The contribution of Fig. 1i is expressed as

$$\Gamma_i^{\mu(p)} = \frac{4\mathcal{C}^2}{3} \frac{4m_\Delta^2+c_1Q^2}{4m_\Delta^2+Q^2} I_{i\pi}^{N\Delta} + \frac{\mathcal{C}^2}{6} \frac{4m_\Sigma^{*2}+c_1Q^2}{4m_\Sigma^{*2}+Q^2} I_{iK}^{N\Sigma^*}, \quad (48)$$

$$\Gamma_i^{\mu(n)} = -\frac{\mathcal{C}^2}{3} \frac{4m_\Delta^2 + c_1 Q^2}{4m_\Delta^2 + Q^2} I_{i\pi}^{N\Delta} - \frac{\mathcal{C}^2}{6} \frac{4m_{\Sigma^*}^2 + c_1 Q^2}{4m_{\Sigma^*}^2 + Q^2} I_{iK}^{N\Sigma^*}, \quad (49)$$

where

$$\begin{aligned} I_{i\pi}^{N\Delta} &= \bar{u}(p') \int \frac{d^4 k}{(2\pi)^4} \frac{1}{2f^2} (k_\sigma + z \not{k} \gamma_\sigma) F(k) \frac{1}{D_\pi(k)} \frac{1}{\not{p}' - \not{k} - m_\Delta} S_{\sigma\alpha} \\ &\times (-2\gamma^{\alpha\beta\mu}) \frac{1}{\not{p} - \not{k} - m_\Delta} S_{\beta\rho} (-k_\rho - z \gamma_\rho \not{k}) F(k) u(p). \end{aligned} \quad (50)$$

The contribution of Fig. 1j is expressed as

$$\Gamma_j^{\mu(p)} = \frac{4\mathcal{C}^2}{3} I_{j\pi}^{N\Delta} + \frac{\mathcal{C}^2}{6} I_{jK}^{N\Sigma^*}, \quad (51)$$

$$\Gamma_j^{\mu(n)} = -\frac{\mathcal{C}^2}{3} I_{j\pi}^{N\Delta} - \frac{\mathcal{C}^2}{6} I_{jK}^{N\Sigma^*}, \quad (52)$$

where

$$\begin{aligned} I_{j\pi}^{N\Delta} &= \bar{u}(p') \int \frac{d^4 k}{(2\pi)^4} \frac{1}{2f^2} (k_\sigma + z \not{k} \gamma_\sigma) F(k) \frac{i}{D_\pi(k)} \frac{i}{\not{p}' - \not{k} - m_\Delta} S_{\sigma\nu} \frac{(1 - c_1)}{m_\Delta} \sigma^{\mu\lambda} q_\lambda \\ &\times \frac{i}{\not{p} - \not{k} - m_\Delta} S_{\nu\rho} (-k_\rho - z \gamma_\rho \not{k}) F(k) u(p). \end{aligned} \quad (53)$$

The contribution of Fig. 1k+1l is expressed as

$$\Gamma_{k+l}^{\mu(p)} = 2(D + F) \mathcal{C} I_{(k+l)\pi}^{N\Delta} + \frac{5}{4} (D - F) \mathcal{C} I_{(k+l)K}^{\Sigma\Sigma^*} + \frac{1}{4} (3F + D) \mathcal{C} I_{(k+l)K}^{\Lambda\Sigma^*}, \quad (54)$$

$$\Gamma_{k+l}^{\mu(n)} = -2(D + F) \mathcal{C} I_{(k+l)\pi}^{N\Delta} + \frac{1}{4} (D + F) \mathcal{C} I_{(k+l)K}^{\Sigma\Sigma^*} - \frac{1}{4} (3F + D) \mathcal{C} I_{(k+l)K}^{\Lambda\Sigma^*}, \quad (55)$$

where

$$\begin{aligned} I_{(k+l)\pi}^{\Sigma\Sigma^*} &= -F(q) \bar{u}(p') \int \frac{d^4 k}{(2\pi)^4} \frac{c_1}{6m_{\Sigma^*} f^2} F^2(k) \not{k} \gamma_5 \frac{1}{\not{p}' - \not{k} - m_\Sigma} \gamma^\nu \gamma_5 q_\nu \frac{1}{\not{p} - \not{k} - m_{\Sigma^*}} S_{\mu\rho} (k_\rho + z \gamma_\rho \not{k}) \frac{i}{D_\pi(k)} u(p) \\ &+ F(q) \bar{u}(p') \int \frac{d^4 k}{(2\pi)^4} \frac{c_1}{6m_{\Sigma^*} f^2} F^2(k) \not{k} \gamma_5 \frac{1}{\not{p}' - \not{k} - m_\Sigma} \gamma^\mu \gamma_5 q_\mu \frac{1}{\not{p} - \not{k} - m_{\Sigma^*}} S_{\nu\rho} (k_\rho + z \gamma_\rho \not{k}) \frac{i}{D_\pi(k)} u(p) \\ &- F(q) \bar{u}(p') \int \frac{d^4 k}{(2\pi)^4} \frac{c_1}{6m_{\Sigma^*} f^2} F^2(k) (k_\nu + z \not{k} \gamma_\nu) \frac{1}{\not{p}' - \not{k} - m_\Sigma} S_{\nu\rho} q_\rho \gamma^\mu \gamma_5 \frac{1}{\not{p} - \not{k} - m_{\Sigma^*}} \not{k} \gamma_5 \frac{1}{D_\pi(k)} u(p) \\ &+ F(q) \bar{u}(p') \int \frac{d^4 k}{(2\pi)^4} \frac{c_1}{6m_{\Sigma^*} f^2} F^2(k) (k_\nu + z \not{k} \gamma_\nu) \frac{1}{\not{p}' - \not{k} - m_\Sigma} S_{\nu\mu} q_\mu \gamma^\rho \gamma_5 \frac{1}{\not{p} - \not{k} - m_{\Sigma^*}} \not{k} \gamma_5 \frac{1}{D_\pi(k)} u(p). \end{aligned} \quad (56)$$

The contribution of Fig. 1m+1n is expressed as

$$\Gamma_{m+n}^{\mu(p)} = \frac{2\mathcal{C}^2}{3} I_{(m+n)\pi}^{N\Delta} - \frac{\mathcal{C}^2}{6} I_{(m+n)K}^{N\Sigma^*}, \quad (57)$$

$$\Gamma_{m+n}^{\mu(n)} = -\frac{2\mathcal{C}^2}{3} I_{(m+n)\pi}^{N\Delta} - \frac{\mathcal{C}^2}{3} I_{(m+n)K}^{N\Sigma^*}, \quad (58)$$

where

$$\begin{aligned} I_{(m+n)\pi}^{N\Delta} &= eF(q) \bar{u}(p') \int \frac{d^4 k}{(2\pi)^4} \frac{1}{2f^2} (k_\sigma + z \not{k} \gamma_\sigma) F(k) \frac{1}{D_\pi(k)} \frac{1}{\not{p}' - \not{k} - m_\Delta} S_{\sigma\rho} (g^{\rho\mu} + z \gamma^\rho \gamma^\mu) F(-k + q) u(p) \\ &+ eF(q) \bar{u}(p') \int \frac{d^4 k}{(2\pi)^4} \frac{1}{2f^2} (g^{\sigma\mu} + z \gamma^\mu \gamma^\sigma) F(k + q) \frac{1}{D_\pi(k)} \frac{1}{\not{p} - \not{k} - m_\Delta} S_{\sigma\rho} F(k) (k_\rho + z \gamma_\rho \not{k}) u(p). \end{aligned} \quad (59)$$

The contribution of Fig. 1o+1p is expressed as

$$\Gamma_{o+p}^{\mu(p)} = \frac{2\mathcal{C}^2}{3} I_{(o+p)\pi}^{N\Delta} - \frac{\mathcal{C}^2}{6} I_{(o+p)K}^{N\Sigma^*}, \quad (60)$$

$$\Gamma_{o+p}^{\mu(n)} = -\frac{2\mathcal{C}^2}{3} I_{(o+p)\pi}^{N\Delta} - \frac{\mathcal{C}^2}{3} I_{(o+p)K}^{N\Sigma^*}, \quad (61)$$

where

$$\begin{aligned} I_{(o+p)\pi}^{N\Delta} = & -eF(q) \bar{u}(p') \int \frac{d^4k}{(2\pi)^4} \frac{1}{2f^2} (k_\sigma + z\mathbb{k}\gamma_\sigma) F(k) \frac{1}{D_\pi(k)} \frac{1}{\not{p}' - \mathbb{k} - m_\Delta} S_{\sigma\rho}(k_\rho + z\gamma_\rho \mathbb{k}) \\ & \times \frac{(-2k+q)^\mu}{-2kq+q^2} [F(k-q) - F(k)] u(p) \\ & + eF(q) \bar{u}(p') \int \frac{d^4k}{(2\pi)^4} \frac{1}{2f^2} (k_\sigma + z\mathbb{k}\gamma_\sigma) \frac{(2k+q)^\mu}{2kq+q^2} [F(k+q) - F(k)] \\ & \times \frac{1}{D_\pi(k)} \frac{1}{\not{p} - \mathbb{k} - m_\Delta} S_{\sigma\rho} F(k) (k_\rho + z\gamma_\rho \mathbb{k}) u(p). \end{aligned} \quad (62)$$

-
- [1] D.-H. Lu, A. W. Thomas, and A. G. Williams, Phys. Rev. **C57**, 2628 (1998), nucl-th/9706019.
 - [2] K. Berger, R. F. Wagenbrunn, and W. Plessas, Phys. Rev. **D70**, 094027 (2004), nucl-th/0407009.
 - [3] B. Julia-Diaz, D. O. Riska, and F. Coester, Phys. Rev. **C69**, 035212 (2004), [Erratum: Phys. Rev. **C75**, 069902(2007)], hep-ph/0312169.
 - [4] A. J. Buchmann and R. F. Lebed, Phys. Rev. **D67**, 016002 (2003), hep-ph/0207358.
 - [5] S. Cheedket, V. E. Lyubovitskij, T. Gutsche, A. Faessler, K. Pumsa-ard, and Y. Yan, Eur. Phys. J. **A20**, 317 (2004), hep-ph/0212347.
 - [6] R. A. Williams and C. Puckett-Truman, Phys. Rev. **C53**, 1580 (1996).
 - [7] P.-N. Shen, Y.-B. Dong, Z.-Y. Zhang, Y.-W. Yu, and T. S. H. Lee, Phys. Rev. **C55**, 2024 (1997).
 - [8] R. Jakob, P. Kroll, M. Schurmann, and W. Schweiger, Z. Phys. **A347**, 109 (1993), hep-ph/9310227.
 - [9] G. Hellstern and C. Weiss, Phys. Lett. **B351**, 64 (1995), hep-ph/9502217.
 - [10] J. M. Zanotti, D. B. Leinweber, A. G. Williams, and J. B. Zhang, Nucl. Phys. Proc. Suppl. **129**, 287 (2004), [287(2003)], hep-lat/0309186.
 - [11] S. Boinpalli, D. B. Leinweber, A. G. Williams, J. M. Zanotti, and J. B. Zhang, Phys. Rev. **D74**, 093005 (2006), hep-lat/0604022.
 - [12] C. Alexandrou, G. Koutsou, J. W. Negele, and A. Tsapalis, Phys. Rev. **D74**, 034508 (2006), hep-lat/0605017.
 - [13] M. Gockeler, T. R. Hemmert, R. Horsley, D. Pleiter, P. E. L. Rakow, A. Schafer, and G. Schierholz (QCDSF), Phys. Rev. **D71**, 034508 (2005), hep-lat/0303019.
 - [14] M. Gockeler et al. (QCDSF/UKQCD), PoS **LAT2007**, 161 (2007), 0710.2159.
 - [15] R. G. Edwards, G. T. Fleming, P. Hagler, J. W. Negele, K. Orginos, A. V. Pochinsky, D. B. Renner, D. G. Richards, and W. Schroers (LHPC), PoS **LAT2005**, 056 (2006), hep-lat/0509185.
 - [16] C. Alexandrou et al. (Lattice Hadron), J. Phys. Conf. Ser. **16**, 174 (2005).
 - [17] T. Fuchs, J. Gegelia, and S. Scherer, J. Phys. **G30**, 1407 (2004), nucl-th/0305070.
 - [18] B. Kubis and U.-G. Meissner, Nucl. Phys. **A679**, 698 (2001), hep-ph/0007056.
 - [19] R. D. Young, D. B. Leinweber, and A. W. Thomas, Prog. Part. Nucl. Phys. **50**, 399 (2003), [399(2002)], hep-lat/0212031.
 - [20] D. B. Leinweber, A. W. Thomas, and R. D. Young, Phys. Rev. Lett. **92**, 242002 (2004), hep-lat/0302020.
 - [21] P. Wang, D. B. Leinweber, A. W. Thomas, and R. D. Young, Phys. Rev. **D75**, 073012 (2007), hep-ph/0701082.
 - [22] P. Wang and A. W. Thomas, Phys. Rev. **D81**, 114015 (2010), 1003.0957.
 - [23] C. R. Allton, W. Armour, D. B. Leinweber, A. W. Thomas, and R. D. Young, Phys. Lett. **B628**, 125 (2005), hep-lat/0504022.
 - [24] W. Armour, C. R. Allton, D. B. Leinweber, A. W. Thomas, and R. D. Young, Nucl. Phys. **A840**, 97 (2010), 0810.3432.
 - [25] J. M. M. Hall, D. B. Leinweber, and R. D. Young, Phys. Rev. **D88**, 014504 (2013), 1305.3984.
 - [26] D. B. Leinweber, S. Boinpalli, I. C. Cloet, A. W. Thomas, A. G. Williams, R. D. Young, J. M. Zanotti, and J. B. Zhang, Phys. Rev. Lett. **94**, 212001 (2005), hep-lat/0406002.
 - [27] P. Wang, D. B. Leinweber, A. W. Thomas, and R. D. Young, Phys. Rev. **C79**, 065202 (2009), 0807.0944.
 - [28] P. Wang, D. B. Leinweber, A. W. Thomas, and R. D. Young, Phys. Rev. **D86**, 094038 (2012), 1210.5072.
 - [29] P. Wang, D. B. Leinweber, and A. W. Thomas, Phys. Rev. **D89**, 033008 (2014), 1312.3375.
 - [30] J. M. M. Hall, D. B. Leinweber, and R. D. Young, Phys. Rev. **D89**, 054511 (2014), 1312.5781.
 - [31] P. Wang, D. B. Leinweber, and A. W. Thomas, Phys. Rev. **D92**, 034508 (2015), 1504.06392.
 - [32] H. Li, P. Wang, D. B. Leinweber, and A. W. Thomas, Phys. Rev. **C93**, 045203 (2016), 1512.02354.

- [33] H. Li and P. Wang, Chin. Phys. **C40**, 123106 (2016), 1608.03111.
- [34] P. Wang, D. B. Leinweber, A. W. Thomas, and R. D. Young, Phys. Rev. **D79**, 094001 (2009), 0810.1021.
- [35] E. E. Jenkins, Nucl. Phys. **B368**, 190 (1992).
- [36] E. E. Jenkins, M. E. Luke, A. V. Manohar, and M. J. Savage, Phys. Lett. **B302**, 482 (1993), [Erratum: Phys. Lett. **B388**, 866(1996)], hep-ph/9212226.
- [37] S. Scherer, Adv. Nucl. Phys. **27**, 277 (2003), hep-ph/0210398.
- [38] J. Terning, Phys. Rev. **D44**, 887 (1991).
- [39] Amand Faessler, T. Gutsche, M. A. Ivanov, V. E. Lyubovitskij, P. Wang, Phys. Rev. **D68**, 014011 (2003).
- [40] P. Wang, Can. J. Phys. **92**, 25 (2014).
- [41] V. Pascalutsa, M. Vanderhaeghen, and S. N. Yang, Phys. Rept. **437**, 125 (2007), hep-ph/0609004.
- [42] L. M. Nath, B. Etemadi, and J. D. Kimel, Phys. Rev. **D3**, 2153 (1971).
- [43] M. Seimetz (A1), Nucl. Phys. **A755**, 253 (2005).
- [44] M. Ostrick, Eur. Phys. J. **A28S1**, 81 (2006).
- [45] S. Riordan et al., Phys. Rev. Lett. **105**, 262302 (2010), 1008.1738.